

## ARTICLES

## Enhancing the Performance of a Supported Titanium Epoxidation Catalyst by Modifying the Active Center

Richard D. Oldroyd,<sup>\*,†</sup> Gopinathan Sankar,<sup>†</sup> John Meurig Thomas,<sup>\*,†,‡</sup> and Dogan Özkaya<sup>‡</sup>*Davy-Faraday Research Laboratory, The Royal Institution of Great Britain, 21 Albemarle Street, London W1X 4BS, U.K., and Department of Materials Science and Metallurgy, University of Cambridge, Pembroke Street, Cambridge CB2 3QZ, U.K.**Received: May 16, 1997; In Final Form: December 2, 1997*

Significant effects on catalytic activity in the epoxidation of cyclohexene with alkyl hydroperoxides are observed when the surface of mesoporous silica (MCM-41) is modified with either Ge(IV) or Sn(IV) prior to the grafting of tetracoordinated Ti(IV). Titanium centers attached via oxygen to two silicons and one germanium show an increase in turnover frequency of up to 140% compared to centers attached via three Si–O bonds to a purely siliceous MCM-41. The tin-modified catalyst, in contrast, shows poor activity. The environments of the Ti, Ge, and Sn centers were probed directly by in situ X-ray absorption spectroscopy and also by ex situ transmission electron microscopy. The germanium-modified silica contains evenly distributed, anchored tetrahedral Ge(IV) species, whereas the tin-containing material forms extraframework particles of SnO<sub>2</sub>.

## Introduction

For a variety of reasons great effort is currently being directed toward the study of heterogeneous Ti(IV) catalysts.<sup>1–7</sup> First, there is their high activity and selectivity in catalyzing various oxidations, such as the industrial conversion of propene to propene oxide. Second, the titanasilicate TS-1, based on Ti(IV) substituted silicalite-1, is now in commercial use in a variety of reactions, including the conversion of styrene to its epoxide,<sup>7,8</sup> although it can oxidize only relatively small molecules because of pore-size limitations. But there are many other viable selective oxidation reactions catalyzed by Ti(IV) embedded in silica.<sup>9–15</sup> The past three years have seen increasing use of MCM-41 mesoporous silica as a support for Ti(IV) centers, the interest arising mainly from its high surface area and large pores (>15 Å diameter),<sup>16</sup> which make it accessible, in a potentially shape-selective mode, to large and bulky molecules.<sup>17</sup> Two main types of Ti(IV)-modified MCM-41 materials have hitherto been highlighted: one where Ti(IV) centers are distributed throughout the MCM-41 structure (designated Ti → MCM-41)<sup>9–12</sup> by addition of a suitable Ti(IV) precursor to the MCM-41 synthesis gel; the other where titanium, by use of an organometallic precursor, is grafted onto the MCM-41 surface (designated Ti†MCM-41).<sup>15</sup> There are considerable advantages in using the latter method to produce supported catalysts because of the greater accessibility of the grafted metal centers to the reactants. Indeed, some of us have shown<sup>18</sup> in a recent investigation that Ti†MCM-41 is 10 times as active toward cyclohexene epoxidation as Ti → MCM-41.

In the work presented here we show how the activity of Ti†MCM-41 may be significantly altered by prior modification of the surface of the MCM-41, achieved by grafting tetrabutyl

germanium (Bu<sub>4</sub>Ge) and tetrabutyl tin (Bu<sub>4</sub>Sn) onto the surface of the support, before introducing the Ti(IV) centers. A combination of X-ray absorption spectroscopy (XAS), transmission electron microscopy (TEM), IR spectroscopy, and X-ray diffraction was used to characterize the structures of the resulting materials, the catalytic activity of which toward cyclohexene epoxidation, in the presence of either *tert*-butyl hydroperoxide (TBHP) or cumene hydroperoxide (CuHP), is also reported.

## Experimental Section

**MCM-41 Synthesis.** The procedure of Rey et al. was adopted,<sup>13</sup> using Degussa Aerosil silica, tetramethylammonium hydroxide (TMAOH), hexadecyltrimethylammonium bromide (C<sub>16</sub>NBr), and water in molar ratios of 1:0.26:0.70:25. The C<sub>16</sub>-NBr was added to the TMAOH and water followed by slow addition of the silica under constant stirring. The gel was transferred to a polypropylene container, sealed and heated to 90 °C for 16 h. The resulting material was filtered off, washed with copious amounts of water, and calcined under nitrogen at 550 °C for 1 h followed by 6 h under oxygen at the same temperature.

**Ge and Sn Modification of MCM-41.** MCM-41 (2 g) was dehydrated at 200 °C under vacuum for ca. 2 h and subsequently treated with either Bu<sub>4</sub>Ge (10 mL, 180 °C) or Bu<sub>4</sub>Sn (10 mL, 80 °C) for a minimum of 16 h under a dry argon atmosphere, based on the procedures reported by Nédéz et al. for analogous silica-supported materials.<sup>19,20</sup> After filtration and thorough washing with 300 mL of diethyl ether, the materials were calcined in oxygen at 550 °C for ca. 2 h to form the Ge(IV)- and Sn(IV)-modified materials (designated Ge†MCM-41 and Sn†MCM-41, respectively).

**Titanium Grafting.** A 2 g sample of either siliceous MCM-41, Ge†MCM-41, Sn†MCM-41 or Degussa Aerosil 200

<sup>†</sup> The Royal Institution of Great Britain.<sup>‡</sup> University of Cambridge.

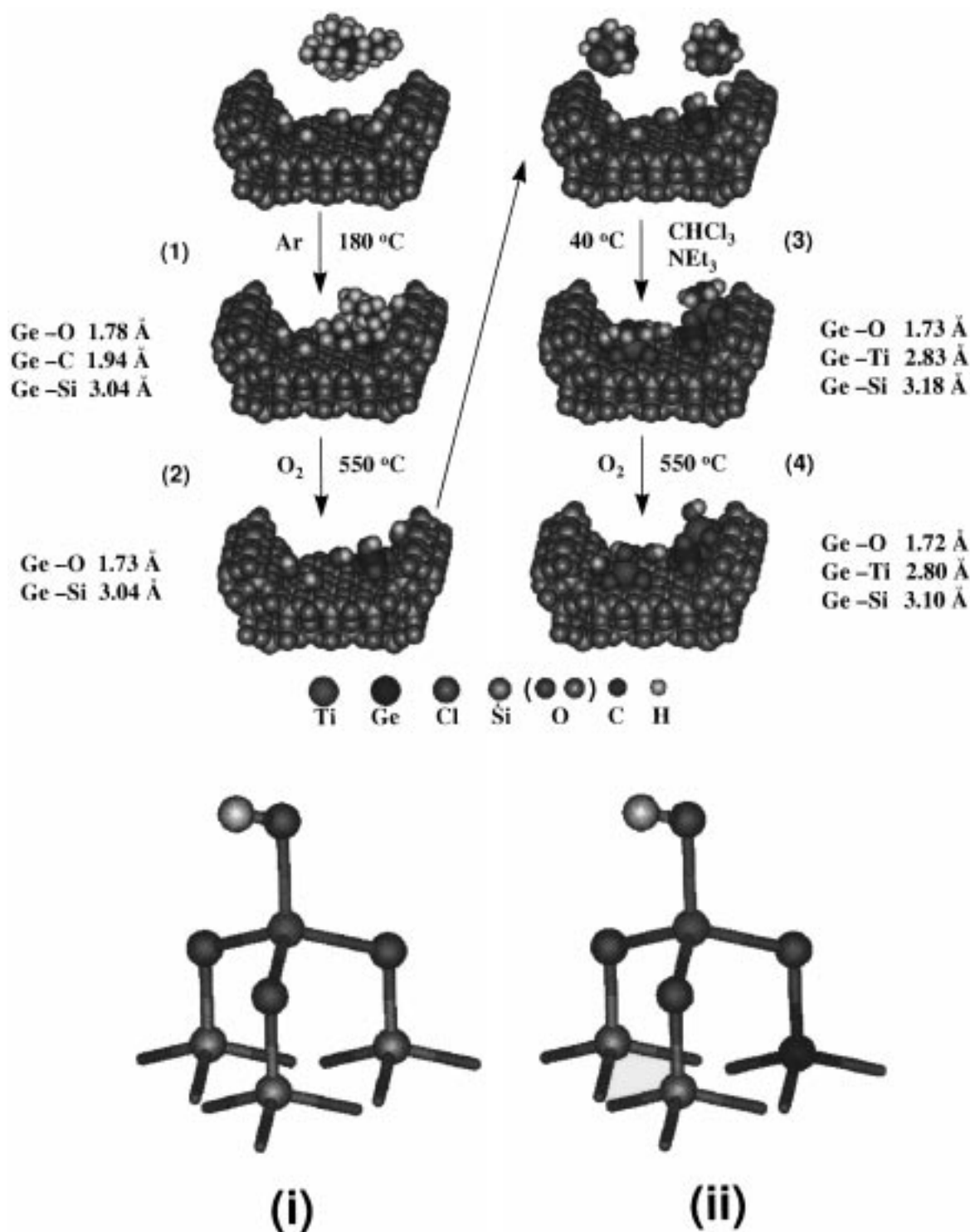


**Figure 1.** (a, top) Steps involved in synthesizing Ti/Ge/MCM-41: (1) reaction of tetrabutylgermanium with a mesoporous MCM-41 silica surface; (2) calcination of the resultant tributyl germanium moieties to form pendant Ge–OH groups; (3) reaction of TiCp<sub>2</sub>Cl<sub>2</sub> with the mesoporous surface containing pendant Ge–OH and Si–OH species; (4) calcination to yield a surface containing a mixture of Ti–OH supported to three O–Si groups and Ti–OH supported to one O–Ge and two O–Si groups. For clarity, the oxygen atoms of the MCM-41 support are shown in light-gray, and most surface ≡Si–OH groups on the surface have been omitted. (b, bottom) Two types of catalytically active titanium environments in Ti/Ge/MCM-41 where Ti–OH moieties are linked to the mesoporous surface via (i) three Ti–O–Si bonds and (ii) one Ti–O–Ge and two Ti–O–Si bonds. The color scheme is the same as in part a.

silica (labeled from now on as SiO<sub>2</sub>) was dehydrated at 200 °C under vacuum for at least 2 h. The sample was then stirred in a solution of TiCp<sub>2</sub>Cl<sub>2</sub> dissolved in 75 mL of anhydrous chloroform under a dry argon atmosphere at 40 °C. After 30 min 1 mL of NEt<sub>3</sub> was added and the mixture then stirred under the same conditions for 16 h. The resulting yellow material was filtered off, washed with 300 mL of chloroform and calcined

in oxygen as described above.<sup>15</sup> The catalysts were synthesized to yield a Ti:Si ratio of ca. 1:50.

**Catalysis.** Catalytic tests were performed under argon at 30 °C using 50 mg of catalyst, 2 mL of cyclohexene, 0.5 mL of TBHP (or 0.7 mL of CuHP), and enough acetonitrile to make the total volume 9.5 mL. Reactions were quenched after 1 h using triphenylphosphine, and 0.5 mL of mesitylene was added

as an internal GC standard. Time-resolved studies were performed at the same temperature and also under argon by employing 75 mg of catalyst, 2 mL of cyclohexene, 1 mL of TBHP, 0.5 mL of mesitylene (as a GC standard), and 6.5 mL of acetonitrile. Aliquots of 0.1 mL were periodically removed from the reaction vessel and filtered through a 0.2- $\mu\text{m}$  syringe filter to remove the catalyst, and the filtrate was analyzed by GC. Reagents, solvents, and catalyst were used without any predrying or purification. No oxidation was observed after removal of the catalysts. The supports themselves (i.e.,  $\text{SiO}_2$ , MCM-41, Ge $\dagger$ MCM-41, and Sn $\dagger$ MCM-41) were shown to be inactive toward catalysis.

**Data Collection.** X-ray absorption spectra at the Ti, Ge, and Sn K-edges were collected, by use of an in situ cell,<sup>21</sup> on stations 8.1 and 9.2 of the Daresbury Laboratory operating with an energy of 2 GeV and an average beam current of ca. 200 mA. The incident intensity was measured using an Ar/He-filled ion chamber, and the fluoresced X-rays were detected using a Canberra 13-element solid-state detector. XRD patterns were collected on a Siemens D500 diffractometer using Cu K $\alpha$  radiation. FTIR spectra of calcined samples were recorded on a Perkin-Elmer 1725X spectrometer using an in situ cell.<sup>21</sup> Transmission electron microscopy was performed using a VG HB 800 scanning transmission electron microscope. Elemental maps were created by analysis of the K-edge X-ray fluorescence for Ti, O, Si, and Ge, with the L-edge being monitored for Sn.

## Results and Discussion

Four catalysts were used in this study, which contained Ti(IV) anchored to (i) siliceous MCM-41, (ii) germanium-modified MCM-41 (Ge $\dagger$ MCM-41), (iii) tin-modified MCM-41 (Sn $\dagger$ MCM-41), or (iv) Degussa Aerosil 200 silica ( $\text{SiO}_2$ ). The Ge $\dagger$ MCM-41 and Sn $\dagger$ MCM-41 supports were synthesized by treating dehydrated MCM-41 with either  $\text{GeBu}_4$  or  $\text{SnBu}_4$  using the procedures of Nédez et al.,<sup>19,20</sup> as amplified in the Experimental Section. After calcination, titanocene dichloride ( $\text{TiCp}_2\text{Cl}_2$ ) was reacted with the dehydrated supports and subsequently calcined in the usual fashion<sup>15</sup> to form the active catalysts. Figure 1 illustrates the steps involved in synthesizing the Ti $\dagger$ Ge $\dagger$ MCM-41 catalyst, as determined by the in situ EXAFS and IR experiments described below.

The initial discussion will concentrate mainly on the TEM and X-ray diffraction work followed by the results arising from X-ray absorption spectroscopy for each element in turn. Finally, the catalytic activity of these materials toward cyclohexene epoxidation will be discussed and comparisons made between the catalysts' structures and their activities.

**Structural Considerations.** Transmission electron micrographs, together with elemental maps produced from electron-stimulated X-ray emission (shown in Figure 2), of the non-titanium-containing supports show that germanium is evenly spread throughout the MCM-41 sample in freshly calcined Ge $\dagger$ MCM-41. The same is true for Sn in Sn $\dagger$ MCM-41. On addition of titanium and subsequent calcination, the germanium is still found, by elemental mapping, to be evenly spread throughout the Ti $\dagger$ Ge $\dagger$ MCM-41 sample. This is not the situation for Ti $\dagger$ Sn $\dagger$ MCM-41 where electron microscopy shows particles of extraframework tin-containing material (Figure 2c), the X-ray diffraction pattern of which exhibits peaks characteristic of the cassiterite phase of  $\text{SnO}_2$  (Figure 3). Evidently the interaction between tin and the silica support is not strong, and aggregation at the surface takes place readily during heat treatment and calcination. (An effect similar to this has been observed previously in Sn-containing silicalites where the tin leaches out

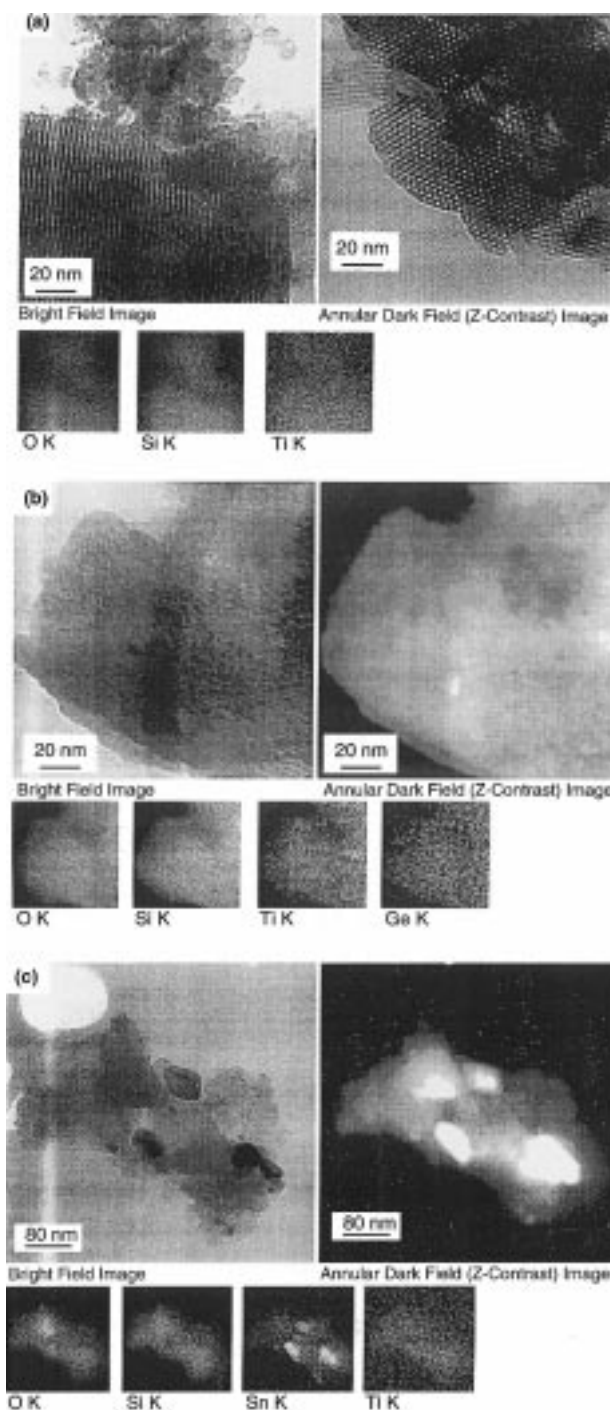


**Figure 2.** Transmission electron micrographs and elemental maps of calcined samples of (a) Ti $\dagger$ MCM-41, (b) Ti $\dagger$ Ge $\dagger$ MCM-41, and (c) Ti $\dagger$ Sn $\dagger$ MCM-41.

of the framework during calcination.)<sup>22</sup> The anchored titanium is, however, evenly spread throughout the catalysts, even on the extraframework  $\text{SnO}_2$  particles on the surface of Ti $\dagger$ Sn $\dagger$ MCM-41.

The Ti, Ge, and Sn K-edge X-ray absorption spectra yielded the local coordination environment around these atoms (see Tables 1–3, with the XANES spectra shown in Figure 4). Typical EXAFS spectra, along with their corresponding Fourier Transforms, are shown in Figure 5.

**Ti K-Edge XAS.** The calcined catalysts all have Ti K-edge XANES spectra characteristic of tetrahedrally coordinated Ti(IV) centers (Figure 4a),<sup>23</sup> with the first shells of four oxygen atoms at ca. 1.82 Å as determined from the EXAFS. Although

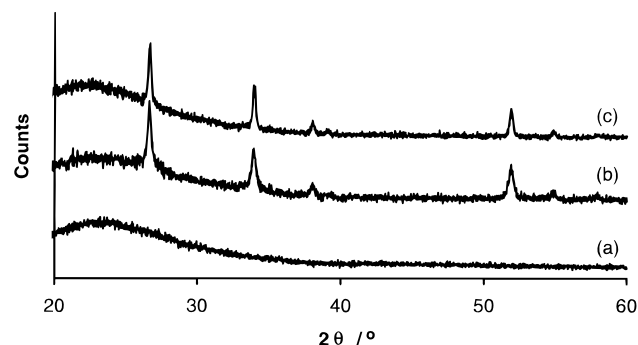


**Figure 3.** X-ray diffraction patterns of (a) calcined SnTiMCM-41, (b) calcined TiTiSnTiMCM-41, and (c) a 3 wt % mixture of SnO<sub>2</sub> and MCM-41.

**TABLE 1: Ti K-Edge EXAFS Data for the Calcined Catalysts**

material	atom type	occupancy	distance Å	2σ <sup>2</sup> Å <sup>2</sup>	Ti—O—Si angle (deg)
TiSiO <sub>2</sub>	O	4.1	1.83	0.009	
	Si	1.9	3.18	0.003	134
	Si	1.2	3.34	0.003	152
TiMCM-41	O	4.1	1.82	0.005	
	Si	2.3	3.19	0.006	138
	Si	0.8	3.37	0.006	160
TiGeMCM-41	O	3.8	1.81	0.002	
	Si	1.7	3.19	0.004	139
	Si	1.1	3.34	0.004	158
TiSnTiMCM-41	O	3.8	1.79	0.005	
	Si	1.7	3.20	0.004	142
	Si	0.9	3.34	0.004	161

**TABLE 2: Ge K-Edge EXAFS Data**

material	atom type	occupancy	distance Å	2σ <sup>2</sup> Å <sup>2</sup>	angle (deg)
GeBu <sub>4</sub>	C	3.5	1.97	0.007	
	C	3.5	2.98	0.021	Ge—C—C: 116
GeMCM-41, uncalcined	O	0.7	1.78	0.003	
	C	3.5	1.94	0.006	
	C	3.5	2.96	0.010	Ge—C—C: 115
GeMCM-41, calcined	Si	0.7	3.04	0.011	Ge—O—Si: 128
	O	3.9	1.73	0.004	
	Si	2.7	3.04	0.005	Ge—O—Si: 132
TiGeMCM-41, calcined	O	4.1	1.72	0.004	
	Ti	0.8	2.80	0.003	Ge—O—Ti: 106
	Si	3.3	3.10	0.003	Ge—O—Si: 136
GeO <sub>2</sub> , (quartz phase)	O	4	1.73	0.008	
	Ge	4	3.17	0.012	Ge—O—Ge: 132
	Ge	2	3.17	0.012	
	O	6	3.39	0.010	
	Ge	6	4.54	0.029	
	Ge	8	5.03	0.030	

it is possible to extract higher shells for all four catalysts, such as two Ti···Si distances, there is no clear evidence from these Ti K-edge EXAFS data for the existence of Ti···Ge and Ti···Sn shells in TiGeMCM-41 and TiSnTiMCM-41, respectively. This is due to the low loadings of Ge and Sn in these materials, which results in the majority of the titanium being anchored to

**TABLE 3: Sn K-Edge EXAFS Data**

material	atom type	occupancy	distance Å	2σ <sup>2</sup> Å <sup>2</sup>	angle (deg)
SnBu <sub>4</sub>	C	4.4	2.17	0.008	
	C	4.4	3.16	0.025	Sn—C—C: 115
SnTiMCM-41, uncalcined	O	1.0	1.99	0.012	
	C	3.1	2.12	0.010	
	C	3.1	3.16	0.021	Sn—C—C: 118
	Si	1.0	3.17	0.009	Sn—O—Si: 123
SnTiMCM-41, calcined	O	4.9	2.00	0.010	
TiSnTiMCM-41, calcined	O	6.0	2.02	0.012	
	Sn	1.2	3.22	0.005	Sn—O—Sn: 105
	Sn	4.8	3.71	0.006	Sn—O—Sn: 131
SnO <sub>2</sub> , (cassiterite phase)	O	6	2.05	0.005	
	Sn	2	3.19	0.005	Sn—O—Sn: 103
	Sn	8	3.72	0.006	Sn—O—Sn: 130
	Sn	4	4.75	0.009	
	Sn	8	5.67	0.009	
	Sn	8	5.92	0.009	
	Sn	6	6.57	0.009	

unmodified regions of the MCM-41. (It should be noted that the data were treated using multiple scattering methods to extract the Ti···Si distances and Ti—O—Si angles following the procedure of Sankar et al.)<sup>24</sup> For titanium grafted on the two purely siliceous supports, it is noteworthy that the intensity of the X-ray absorption pre-edge (1s → 3d) transition is appreciably lower for TiSiO<sub>2</sub> (0.4) than for TiMCM-41 (0.6). This shows that there is significant deviation from tetrahedral coordination in TiSiO<sub>2</sub> resulting from a mixture of both tetrahedral and octahedral sites (a fact that is also corroborated by the large Debye–Waller factor for the Ti—O shell in this material), indicating that the higher surface area of siliceous MCM-41 (1020 ± 10 m<sup>2</sup> g<sup>-1</sup> compared with 200 m<sup>2</sup> g<sup>-1</sup> for Aerosil 200) is able to isolate more effectively tetrahedrally coordinated Ti(IV) centers. The octahedral sites may be attributable to the formation of some microcrystallites of TiO<sub>2</sub> similar to those observed previously for silica-supported titania catalysts.<sup>25</sup>

**Ge K-Edge XAS.** Treatment of MCM-41 silica with Bu<sub>4</sub>-Ge at 180 °C (stage 1 of Figure 1) leads to the average loss of one butyl group forming one Ge—O—Si linkage to the surface, as determined by Ge K-edge EXAFS spectroscopy, and agrees with the original findings of Nédéz et al. based on IR spectroscopy and GC analysis.<sup>19</sup> The Ge—C and Ge—O distances of the bound organogermanium group are all consistent with literature data for tetrahedral Ge(IV) complexes.<sup>26–28</sup> On calcination in oxygen (stage 2 of Figure 1) the organic material is removed, creating tetrahedral Ge(IV) centers bound to the surface via three Ge—O—Si linkages. The Ge—O distances are similar to those found in germanium-containing zeolites.<sup>29</sup> In both uncalcined and calcined TiGeMCM-41 systems, a Ge···Ti distance can be extracted from the Ge K-edge EXAFS at around 2.80 Å (Figure 5b). IR spectroscopy (Figure 6) shows, in addition to the ν({Si}O—H) band at 3747 cm<sup>-1</sup>, a band assignable<sup>30</sup> as a ν({Ge}O—H) stretch at 3680 cm<sup>-1</sup> for calcined GeMCM-41, which almost completely disappears on addi-

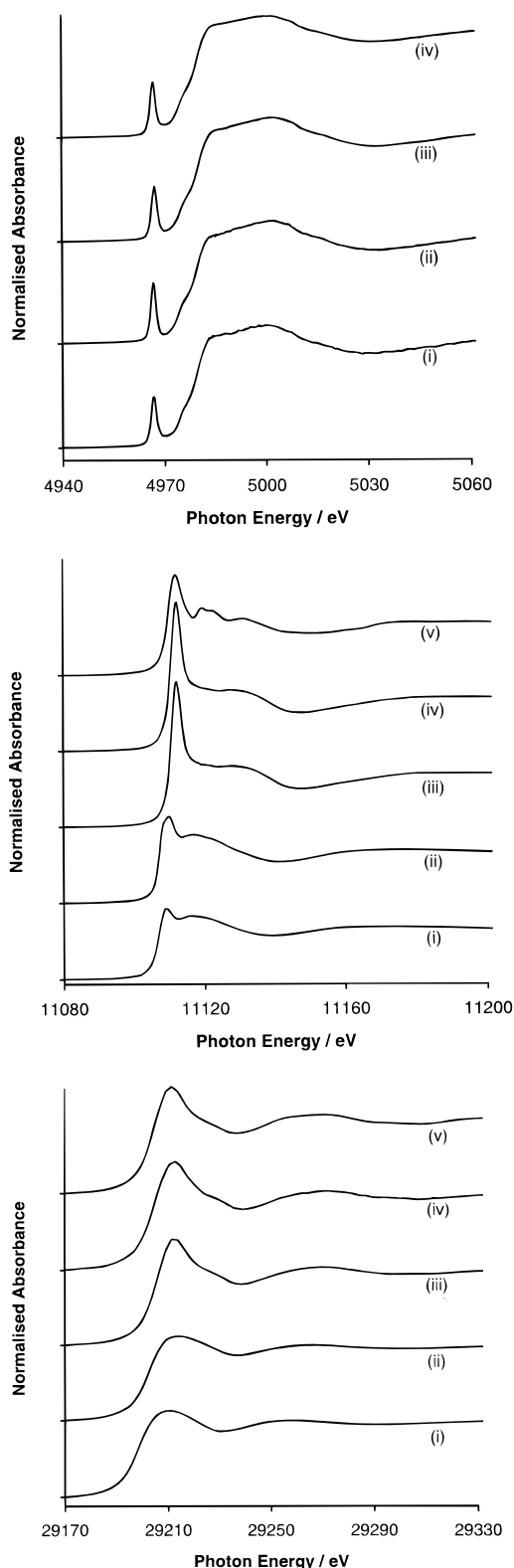


**Figure 4.** (a, top) Ti K-edge XANES spectra of (i)  $\text{Ti}\uparrow\text{SiO}_2$ , (ii)  $\text{Ti}\uparrow\text{MCM-41}$ , (iii)  $\text{Ti}\uparrow\text{Ge}\uparrow\text{MCM-41}$ , and (iv)  $\text{Ti}\uparrow\text{Sn}\uparrow\text{MCM-41}$ ; (b, middle) Ge K-edge XANES spectra of (i)  $\text{Bu}_4\text{Ge}$ , (ii) uncalcined  $\text{Ge}\uparrow\text{MCM-41}$ , (iii) calcined  $\text{Ge}\uparrow\text{MCM-41}$ , (iv) calcined  $\text{Ti}\uparrow\text{Ge}\uparrow\text{MCM-41}$ , (v)  $\text{GeO}_2$  quartz phase; (c, bottom) Sn K-edge XANES spectra of (i)  $\text{Bu}_4\text{Sn}$ , (ii) uncalcined  $\text{Sn}\uparrow\text{MCM-41}$ , (iii) calcined  $\text{Sn}\uparrow\text{MCM-41}$ , (iv) calcined  $\text{Ti}\uparrow\text{Sn}\uparrow\text{MCM-41}$ , (v)  $\text{SnO}_2$  cassiterite phase.

n of the titanium, indicating that almost all the germanium centers present react with the titanium. Simultaneously, a band at ca.  $950\text{ cm}^{-1}$  appears, which is consistent with the formation of  $\text{Ti-O-Si}$  links.<sup>31,32</sup>

**TABLE 4: Results of Cyclohexene Epoxidation Reactions<sup>a</sup>**

catalyst	M:Ti:Si ratio <sup>b</sup>	TBHP turnover frequency to cyclohexene oxide/h <sup>-1 c</sup>	CuHP turnover frequency to cyclohexene oxide/h <sup>-1 d</sup>
$\text{Ti}\uparrow\text{SiO}_2$	0:1:43.6	26.3	27.3
$\text{Ti}\uparrow\text{MCM-41}$	0:1:44.7	33.8	31.2
$\text{Ti}\uparrow\text{Ge}\uparrow\text{MCM-41}$	0.07:1:44.9	39.8	34.4
$\text{Ti}\uparrow\text{Sn}\uparrow\text{MCM-41}$	1.03:1:41.4	12.3	12.9

<sup>a</sup> 50 mg of catalyst, 0.5 mL of TBHP (0.7 mL of CuHP), 2 mL of cyclohexene, 7 mL of acetonitrile (6.8 mL for CuHP reactions), 30 °C, 1 h. <sup>b</sup> M = Ge, Sn. <sup>c</sup> Selectivities to the epoxide are all greater than 80%. Main impurity is cyclohexenol. <sup>d</sup> Selectivities to the epoxide are all greater than 75%. Main impurities are cyclohexenol and cyclohexan-1,2-diol.

These data clearly show that almost all of the germanium atoms on the surface react with titanium during the grafting process (stage 3, Figure 1). It is noteworthy that there is no evidence for the formation of extraframework  $\text{GeO}_2$  phases, either by EXAFS or X-ray diffraction, in  $\text{Ti}\uparrow\text{Ge}\uparrow\text{MCM-41}$ .

**Sn K-Edge XAS.** Analysis of the Sn K-edge EXAFS spectrum obtained from the uncalcined  $\text{Sn}\uparrow\text{MCM-41}$  sample shows that, as with its germanium analogue and again consistent with the initial reports of Nédez et al.,<sup>20</sup> a single butyl ligand is lost to form one  $\text{Sn-O-Si}$  link to the surface with bond distances comparable to those of model systems.<sup>33,34</sup> On calcination, however, isolated tetrahedral  $\text{Sn(IV)}$  centers are not uniquely formed. The best fit to the Sn K-edge EXAFS data was for a single shell of ca. five oxygen atoms, but the reality is almost certainly a mixture of some tetrahedral centers interspersed with dimeric and oligomeric  $\text{Sn-O-Sn}$  species. The Sn K-edge XANES spectrum (Figure 4c) clearly resembles that of the cassiterite phase of  $\text{SnO}_2$ , as does the spectrum of calcined  $\text{Ti}\uparrow\text{Sn}\uparrow\text{MCM-41}$ , which, as described above, shows characteristic  $\text{SnO}_2$  peaks in the X-ray diffraction pattern. The Sn K-edge Fourier transform of  $\text{Ti}\uparrow\text{Sn}\uparrow\text{MCM-41}$  showed a significant reduction in intensity of the tin shells at greater than 3 Å, compared to the tin oxide standard, and is reflected in the correspondingly lower occupancies of these shells obtained when fitting the data.

**Catalysis.** The results of cyclohexene epoxidation by either TBHP or CuHP in the presence of the titanium catalysts are shown in Table 4. Comparing the different catalysts, it is seen that  $\text{Ti}\uparrow\text{Ge}\uparrow\text{MCM-41}$  is the most active with an absolute increase in turnover frequency of approximately 15% over  $\text{Ti}\uparrow\text{MCM-41}$ . This increase is rather large, especially when account is taken of the very low germanium loading of this catalyst—only 0.15 wt %, giving a Ge: Ti molar ratio of 0.07:1. If we assume that 7% of the  $\text{Ti(IV)}$  centers are actually attached to germanium (consistent with the IR and EXAFS spectra that show that almost all the Ge centers are bound via oxygen to titanium), then the actual improvement in activity of these Ge-attached centers, compared to those centers supported on a purely siliceous MCM-41 surface, is as high as 140% using TBHP and 80% with CuHP.

A previous report<sup>35</sup> by Sheldon et al. showed that a much worse selectivity resulted if CuHP was used as the organic hydroperoxide instead of TBHP in the  $\text{TiO}_2/\text{SiO}_2$ -catalyzed epoxidation of allyl chloride. Although in this case the selectivity toward cyclohexene oxide is slightly lower, and some ring opening of the epoxide is apparent, CuHP still functions as an effective oxidizing agent with an efficiency comparable to that of TBHP. The much lower cost of CuHP compared with that of TBHP makes this an attractive alternative for use in practical applications of such reactions.

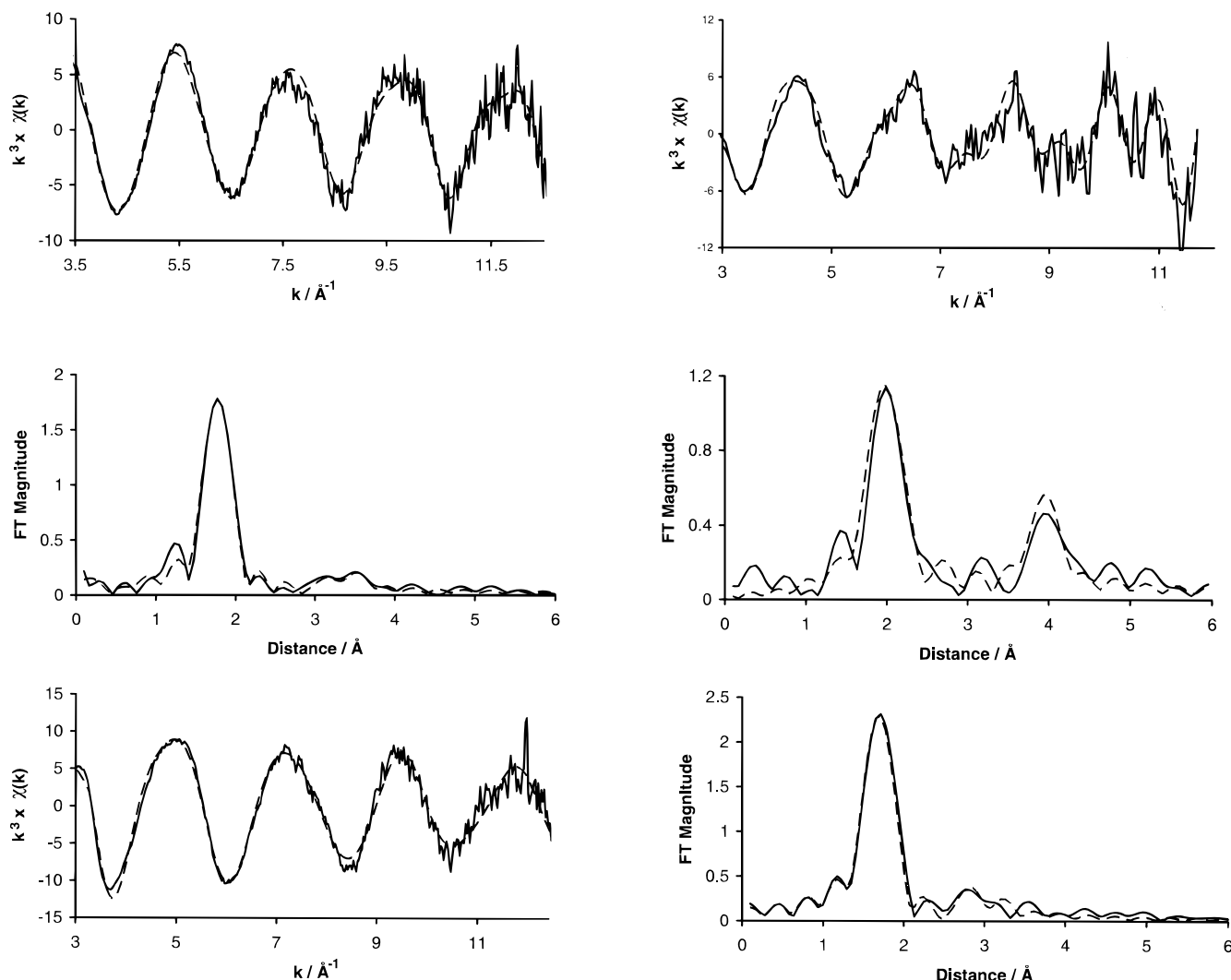


**Figure 5.** EXAFS spectra and associated Fourier transforms: (a, left, top and middle) Ti K-edge of calcined  $\text{Ti}^\dagger\text{Ge}^\dagger\text{MCM-41}$ ; (b, bottom row) Ge K-edge of calcined  $\text{Ti}^\dagger\text{Ge}^\dagger\text{MCM-41}$ ; (c, right, top and middle) Sn K-edge of calcined  $\text{Ti}^\dagger\text{Sn}^\dagger\text{MCM-41}$ . Full line = experimental spectrum. Dashed line = best fit obtained.

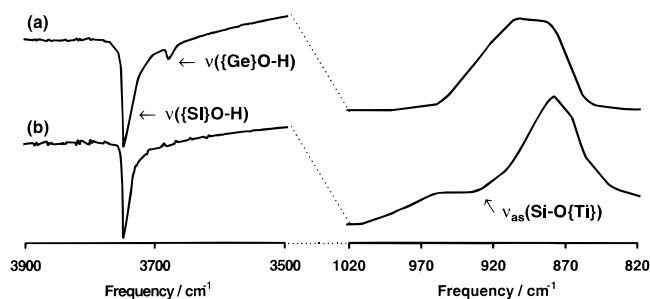


**Figure 6.** IR spectra of freshly calcined (a)  $\text{Ge}^\dagger\text{MCM-41}$  and (b)  $\text{Ti}^\dagger\text{Ge}^\dagger\text{MCM-41}$ .

A  $\text{Ti}^\dagger\text{Ge}^\dagger\text{MCM-41}$  catalyst containing a higher germanium loading could be synthesized using  $\text{Et}_3\text{GeCl}$  as the germanium source. The triethylgermanium chloride was reacted with a dehydrated MCM-41 surface using a procedure analogous to that used for grafting titanocene dichloride onto MCM-41. After calcination (to form  $\text{Ge}^\dagger\text{MCM-41}$ ), reaction with titanocene dichloride, and further calcination, the loading of germanium in this  $\text{Ti}^\dagger\text{Ge}^\dagger\text{MCM-41}$  catalyst was 1.8 wt %, over 10 times the amount contained in the catalyst synthesized using the  $\text{GeBu}_4$  method; yet the catalytic activity of the more heavily loaded material was substantially diminished (to approximately 35% of the cyclohexene conversion achieved by  $\text{Ti}^\dagger\text{MCM-41}$ ), and

the reaction selectivity was substantially altered, with almost equal amounts of cyclohexene oxide and cyclohexan-1,2-diol having been formed after 1 h. This can be explained by the significant number of Ge—OH groups (as shown by the presence of a  $\nu(\{\text{Ge}\}\text{O-H})$  stretch at  $3680 \text{ cm}^{-1}$ ) remaining on the surface of the catalyst that did not react with titanocene dichloride during the Ti-grafting step. These Ge—OH groups are thought to be significantly more acidic than their Si—OH analogues and would therefore be likely to catalyze the ring-opening hydrolysis reaction of epoxide to the diol.

Comparison between titanium centers grafted onto the two purely siliceous supports shows that the  $\text{Ti}^\dagger\text{MCM-41}$  catalyst is superior in activity to the Aerosil supported analogue  $\text{Ti}^\dagger\text{SiO}_2$ . The reasons for this almost certainly stem from the higher surface area of MCM-41 allowing greater dispersion of the Ti(IV) centers and hence reducing the chance of formation of catalytically inactive dimers. This result is consistent with the difference in intensity of the pre-edge Ti K-edge X-ray absorption peaks exhibited by the two materials. There is therefore clearly an advantage in using MCM-41 rather than lower surface-area Aerosil 200 silica as a support.

To explore further the differences between the catalysts, a time-resolved study was undertaken using larger quantities of oxidant and catalyst in order to increase the reaction rate. The

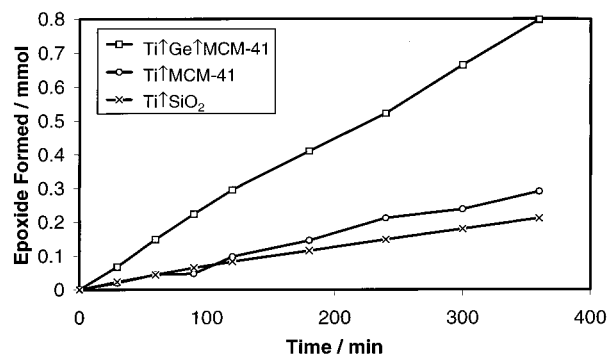


**Figure 7.** Time-resolved profile of cyclohexene oxide production using Ti†Ge†MCM-41, Ti†MCM-41, and Ti†SiO<sub>2</sub> as catalyst and TBHP as oxidant.

results (Figure 7) clearly emphasize the promoting effects of Ge on the titanium catalyst as well as the improvement in activity when using MCM-41 as a support rather than the lower-area Aerosil 200 silica.

The Ti†Sn†MCM-41 shows very poor activity toward epoxidation. This is because the SnO<sub>2</sub> particles formed act as ineffective supports for Ti(IV) centers, as demonstrated by a separate experiment where TiCp<sub>2</sub>Cl<sub>2</sub> was grafted onto high surface-area SnO<sub>2</sub> (synthesized by base hydrolysis of SnCl<sub>4</sub>·5H<sub>2</sub>O using a literature procedure)<sup>36</sup> and subsequently calcined in a fashion analogous to that for the MCM-41-supported samples. The resulting catalyst was totally inactive toward epoxidation.<sup>37</sup> Therefore, in Ti†Sn†MCM-41, any Ti centers that are attached to the extraframework SnO<sub>2</sub> will be deactivated, leaving less titanium attached to the rest of the MCM-41 sample, resulting in a decrease in the overall activity.

## Conclusions

In summary, we have shown that modification of a siliceous MCM-41 surface with tetrahedral Ge(IV) centers, prior to anchoring Ti(IV) tetrahedra, leads to a significant enhancement of catalytic activity toward cyclohexene epoxidation, whereas a catalyst formed from Sn-modified MCM-41 contains extraframework particles of SnO<sub>2</sub> that deactivates the titanium centers and leads to diminished catalytic performance. We have also demonstrated that the cheap and readily available cumene hydroperoxide is an efficient oxidizing agent for the epoxidation of cyclohexene and that the high-surface-area mesoporous silica (MCM-41) is more effective in supporting catalytically active Ti(IV) centers than a lower-surface-area amorphous silica analogue. This work constitutes the basis of a recently filed U.K. patent application.

**Acknowledgment.** We are grateful to the EPSRC for a rolling grant (to J.M.T.) and a ROPA award (R.D.O.) and the Daresbury Laboratory for access to the synchrotron facilities. We also acknowledge use of the EPSRC Chemical Database Service at Daresbury for references to model compounds and stimulating discussions with Dr. T. Maschmeyer.

## References and Notes

- (1) Thomas, J. M. *Philos. Trans. R. Soc. London A* **1990**, 333, 173.
- (2) Thomas, J. M. *Nature* **1994**, 368, 289–90.
- (3) Maxwell, I. E. *Proceedings of the 11th International Congress for Catalysis*, Baltimore, 1996; Bell, A. T., Iglesia, E., Delgass, W. N., Haller, G. L., Eds.; Elsevier: New York, 1996; Vol. A.
- (4) Murugavel, R.; Roesky, H. W. *Angew. Chem., Int. Ed. Engl.* **1997**, 36, 477–479; *Angew. Chem.* **1997**, 109, 491–494.
- (5) Oldroyd, R. D.; Thomas, J. M.; Sankar, G. *Chem. Commun.* **1997**, 2025–2026.
- (6) Ingold, K. U.; Snelgrove, D. W.; MacFaul, P. A.; Oldroyd, R. D.; Thomas, J. M. *Catal. Lett.* **1997**, 48, 21–24.
- (7) Notari, B. *Adv. Catal.* **1996**, 41, 253–334.
- (8) Taramasso, M.; Perego, G.; Notari, B. U.S. Patent 4410501, 1983.
- (9) Tatsumi, T.; Nakamura, M.; Negishi, S.; Tominaga, H. *J. Chem. Soc., Chem. Commun.* **1990**, 476–477.
- (10) Corma, A.; Navarro, M. T.; Pérez Pariente, J. *J. Chem. Soc., Chem. Commun.* **1994**, 147–148.
- (11) Tanev, P. T.; Chibwe, M.; Pinnavaia, T. J. *Nature* **1994**, 368, 321–323.
- (12) Sankar, G.; Rey, F.; Thomas, J. M.; Greaves, G. N.; Corma, A.; Dobson, B. R.; Dent, A. J. *J. Chem. Soc., Chem. Commun.* **1994**, 2279–2280.
- (13) Rey, F.; Sankar, G.; Maschmeyer, T.; Thomas, J. M.; Bell, R. G. *Top. Catal.* **1996**, 3, 121–134.
- (14) Hutter, R.; Mallat, T.; Dutoit, D.; Baiker, A. *Top. Catal.* **1996**, 3, 421–436.
- (15) Maschmeyer, T.; Rey, F.; Sankar, G.; Thomas, J. M. *Nature* **1995**, 378, 159–162.
- (16) Kresge, C. T.; Leonowicz, M. E.; Roth, W. J.; Vartuli, J. C.; Beck, J. S. *Nature* **1992**, 359, 710–712.
- (17) Cambor, M. A.; Corma, A.; Esteve, P.; Martínez, A.; Valencia, S. *Chem. Commun.* **1997**, 795–796.
- (18) Oldroyd, R. D.; Thomas, J. M.; Maschmeyer, T.; MacFaul, P. A.; Snelgrove, D. W.; Ingold, K. U.; Wayner, D. D. M. *Angew. Chem., Int. Ed. Engl.* **1996**, 35, 2787–2790; *Angew. Chem.* **1996**, 108, 2966–2969.
- (19) Nédez, C.; Choplin, A.; Basset, J. M. *Inorg. Chem.* **1994**, 33, 1094–1098.
- (20) Nédez, C.; Theolier, A.; Lefebvre, F.; Choplin, A.; Basset, J. M.; Joly, J. F. *J. Am. Chem. Soc.* **1993**, 115, 722–729.
- (21) Barrett, P. A.; Sankar, G.; Catlow, C. R. A.; Thomas, J. M. *J. Phys. Chem.* **1996**, 100, 8977–8985.
- (22) Fejes, P.; Nagy, J. B.; Kovács, K.; Vankó, G. *Appl. Catal. A* **1996**, 145, 155–184.
- (23) Bordiga, S.; Coluccia, S.; Lamberti, C.; Marchese, L.; Zecchina, A.; Boscherini, F.; Buffa, F.; Genomi, F.; Leofanti, G.; Petrini, G.; Vlaic, G. *J. Phys. Chem.* **1994**, 98, 4125–4132.
- (24) Sankar, G.; Thomas, J. M.; Greaves, G. N.; Dent, A. J. *J. Phys. IV (France)* **1997**, 7, C2-239–C2-240.
- (25) Imamura, S.; Nakai, T.; Kanai, H.; Ito, T. *J. Chem. Soc., Faraday Trans.* **1995**, 91, 1261–1266.
- (26) Puff, H.; Franken, S.; Schuh, W.; Schwab, W. *J. Organomet. Chem.* **1983**, 254, 33–41.
- (27) Puff, H.; Franken, S.; Schuh, W. *J. Organomet. Chem.* **1983**, 256, 23–30.
- (28) Ferguson, G.; Glidewell, C. *Acta Crystollogr., Sect. C* **1996**, 52, 1889–1891.
- (29) Tuilier, M. H.; Lopez, A.; Guth, J. L.; Kessler, H. *Zeolites* **1991**, 11, 662–665.
- (30) Kosslick, H.; Tuan, V. A.; Fricke, R. *Ber. Bunsen-Ges. Phys. Chem.* **1992**, 96, 1761–1765.
- (31) Smirnov, K. S.; van de Graaf, B. *Microporous Mater.* **1996**, 7, 133–138.
- (32) de Man, A. J. M.; Sauer, J. *J. Phys. Chem.* **1996**, 100, 5025–5034.
- (33) Hampden-Smith, M. J.; Wark, T. A.; Rheingold, A.; Huffman, J. C. *Can. J. Chem.* **1991**, 69, 121–129.
- (34) Edelman, M. A.; Hitchcock, P. B.; Lappert, M. F. *J. Chem. Soc., Chem. Commun.* **1990**, 1116–1118.
- (35) Sheldon, R. A.; van Doorn, J. A.; Schram, C. W. A.; de Jong, A. J. *J. Catal.* **1973**, 31, 438–443.
- (36) Hiratsuka, R. S.; Pulcinelli, S. H.; Santilli, C. V. *J. Non-Cryst. Solids* **1990**, 121, 76–83.
- (37) Oldroyd, R. D. Unpublished results.